PROCEEDINGS OF SCIENCE

Measurement of the Z to tau tau cross section with the ATLAS detector

Jana Novakova*
On behalf of the ATLAS Collaboration
Charles University in Prague, Faculty of Mathematics and Physics, Institute of Particle and Nuclear Physics
E-mail: jana.novakova@cern.ch

The Z to tau tau cross section has been measured using data at $\sqrt{s} = 7$ TeV collected with the ATLAS detector at the LHC corresponding to the integrated luminosity of $1.34 - 1.55$ fb^{-1}. The analysis is performed in three different final states determined by decay modes of the tau leptons. Cross sections are measured separately in each final state in a fiducial kinematic phase space and extrapolated to the full phase space in the invariant mass region $66 - 116$ GeV. The individual cross sections are combined together and the product of the total Z boson production cross section and the $Z \to \tau\tau$ branching fraction is measured to be 0.92 ± 0.20 (stat) ± 0.08 (syst) $\pm$ 0.03 (lumi) nb, in agreement with the NNLO theoretical expectations.

36th International Conference on High Energy Physics,
July 4-11, 2012
Melbourne, Australia

*Speaker.

PoS(ICHEP2012)087

1. Introduction

Processes with tau leptons play an important role in searches for new physics phenomena at the LHC. The decay of the Z boson to two tau leptons forms the main background to some of the searches, e.g. $H \to \tau\tau$. Therefore, it is important to measure its production cross section precisely. Furthermore, the cross section measurement of $Z \to \tau\tau$ process is a complementary analysis to the $Z \to ee$ and $Z \to \mu\mu$ precision measurements. Finally, the well known Standard Model processes involving tau leptons are important for the commissioning and validation of τ identification techniques [1] used at the ATLAS experiment [2].

This paper presents the measurement of the $Z \to \tau\tau$ cross section performed in proton-proton collisions at centre of mass energy of 7 TeV. The analysis using dataset from 2011 corresponding to the integrated luminosity of $1.34 - 1.55$ fb^{-1} is documented in Ref. [3]. Three different final states determined by the τ lepton decay modes: $Z \to \tau\tau \to \mu + \text{hadrons} + 3\nu$ (denoted $\tau_\mu\tau_{\text{had}}$ in the following), $Z \to \tau\tau \to e + \text{hadrons} + 3\nu$ (denoted $\tau_e\tau_{\text{had}}$) and $Z \to \tau\tau \to \mu + e + 4\nu$ (denoted $\tau_e\tau_\mu$) are used. The branching fractions given by the PDG are $(22.50 \pm 0.09)\%$, $(23.13 \pm 0.09)\%$ and $(6.20 \pm 0.02)\%$ respectively [4]. Furthermore, the high τ-purity dataset obtained in the $\tau_\mu\tau_{\text{had}}$ channel is used for studies of the distributions of variables relevant for the hadronic τ identification.

2. Event selection

After selecting good collision candidate events, data are required to pass dedicated triggers. The muon trigger with a transverse momentum threshold at 15 GeV and an isolation requirement is used in the $\tau_\mu\tau_{\text{had}}$ and $\tau_e\tau_\mu$ channels, while a combined electron + hadronic tau trigger (with transverse energy cut at 15 GeV on electron + 16 GeV on hadronic tau) in the $\tau_e\tau_{\text{had}}$ channel. Next, exactly one muon candidate (or electron) and a hadronic τ is required in the $\tau_\mu\tau_{\text{had}}$ (or $\tau_e\tau_{\text{had}}$) channel. Similarly, one muon and one electron with opposite charges are looked for in the $\tau_e\tau_\mu$ channel. The transverse momentum threshold is set to 17 GeV for muons and electrons and to 20 (or 25 GeV) for hadronic τ in $\tau_\mu\tau_{\text{had}}$ (or $\tau_e\tau_{\text{had}}$) channel to avoid the turn-on region of the trigger efficiency.

Special cuts reducing the W+jets background are applied. The variables used are motivated by a different event topology in the signal and background events. The variables as defined in the $\tau_\mu\tau_{\text{had}}$ channel are shown bellow (the definitions in the other channels are analogous):

$$\sum \cos(\Delta\phi) = \cos(\phi(\mu) - \phi(E_{\text{T}}^{\text{miss}})) + \cos(\phi(\tau_{\text{had}}) - \phi(E_{\text{T}}^{\text{miss}})) \tag{2.1}$$

$$m_{\text{T}} = \sqrt{2p_{\text{T}}(\mu) \cdot E_{\text{T}}^{\text{miss}} \cdot [1 - \cos\Delta\phi(\mu, E_{\text{T}}^{\text{miss}})]} \tag{2.2}$$

The first variable is used in all three channels and the optimal cut is found to be $\sum\cos(\Delta\phi) > -0.15$. The transverse mass defined in Equation (2.2) is required to be smaller than 50 GeV in the $\tau_\mu\tau_{\text{had}}$ and $\tau_e\tau_{\text{had}}$ channels. The distributions of these variables are shown in Figure 1.

The $t\bar{t}$ background contributes significantly in the $\tau_e\tau_\mu$ channel. Contrary to $Z \to \tau\tau$, $t\bar{t}$ events in the dilepton channel can be characterised by multiple high-p_{T} jets and leptons and large $E_{\text{T}}^{\text{miss}}$. Therefore, events in the $\tau_e\tau_\mu$ channel are required to have $\Sigma_{\text{T}} < 140$ GeV where Σ_{T} is defined as

$$\Sigma_{\text{T}} = p_{\text{T}}(\mu) + E_{\text{T}}(e) + E_{\text{T}}(\text{jets}) + E_{\text{T}}^{\text{miss}}\,. \tag{2.3}$$

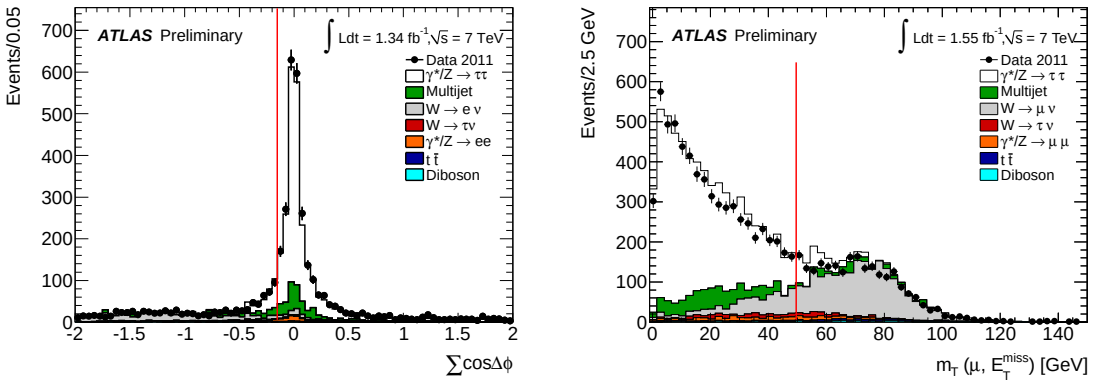

(a) $\tau_e\tau_{\text{had}}$ channel (b) $\tau_\mu\tau_{\text{had}}$ channel

Figure 1: The distributions of (a) $\sum\cos(\Delta\phi)$ in the $\tau_e\tau_{\text{had}}$ channel and (b) m_{T} in the $\tau_\mu\tau_{\text{had}}$ channel [3]. All selection criteria except the cuts on these two variables are applied. The red line indicates the cut value used.

The distribution of Σ_{T} is shown in Figure 2 (a).

Finally, the $Z \to \ell\ell$ background, where ℓ stands for e or μ, is reduced by requiring the invariant mass of the visible parts of the decay (i.e. not considering the neutrinos) to be within the mass window 35 GeV to 75 GeV. While the $Z \to \ell\ell$ events tend to accumulate in the region around 90 GeV, the $Z \to \tau\tau$ signal events peak at around 60 GeV due to the missing energy of the neutrinos. The visible mass distributions for all three channels are shown in Figures 2 (b) and 3 (a), (b).

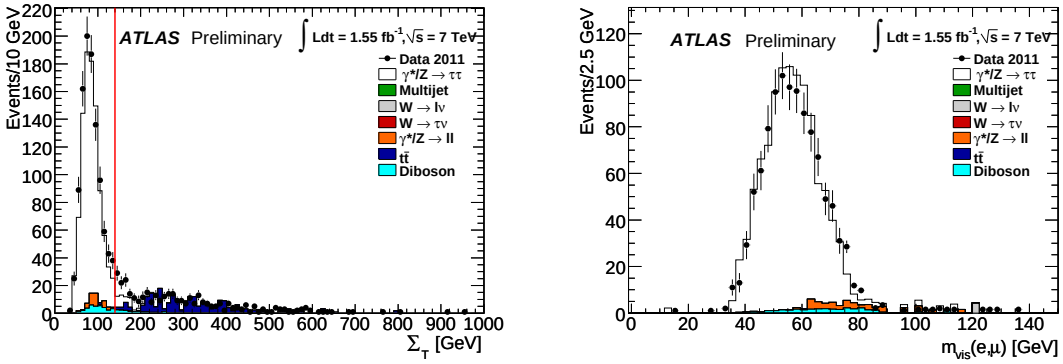

(a) $\tau_e\tau_\mu$ channel (b) $\tau_e\tau_\mu$ channel

Figure 2: The distributions of (a) $\sum_{\text{T}}$ and (b) the visible mass in the $\tau_e\tau_\mu$ channel [3]. All selection criteria except the cut on the plotted variable itself are applied. The red line in (a) indicates the cut value used.

3. Expected number of background events

Contributions of the non-dominant backgrounds ($t\bar{t}$ and dibosons in all three channels and W, Z in the $\tau_e\tau_\mu$ channel) are obtained from Monte Carlo simulations. All other backgrounds (multijet in all three channels and W, Z backgrounds in $\tau_\mu\tau_{\text{had}}$ and $\tau_e\tau_{\text{had}}$ channels) are derived by partially or fully data-driven methods. Normalisation factors are derived in W/Z-enriched control

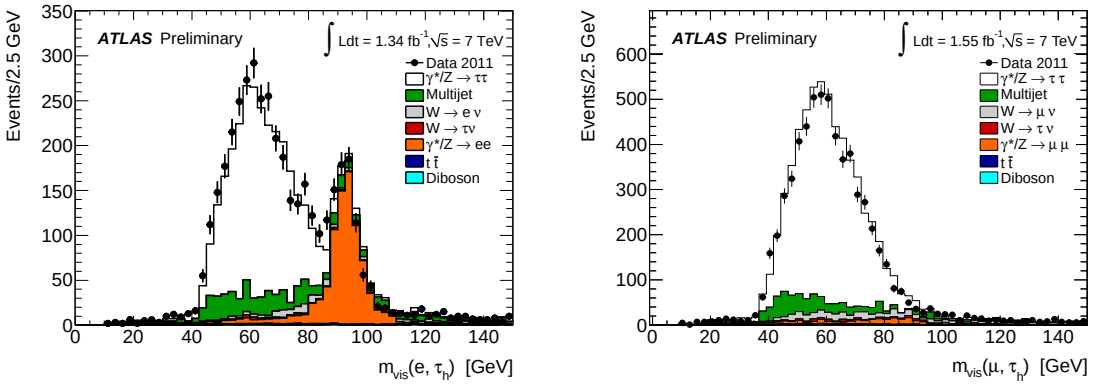

(a) $\tau_e\tau_{\text{had}}$ channel (b) $\tau_\mu\tau_{\text{had}}$ channel

Figure 3: The distributions of the visible mass in the (a) $\tau_e\tau_{\text{had}}$ channel and (b) $\tau_\mu\tau_{\text{had}}$ channel [3]. The contribution of the $Z \to \ell\ell$ background is larger in the $\tau_e\tau_{\text{had}}$ due to the higher fake rate for electrons. All selection criteria except the cut on the visible mass are applied.

regions to correctly scale the Monte Carlo predictions. The multijet background contribution is estimated from the multijet-enriched region with inverse isolation requirement on the lepton and is extrapolated to the signal region. More details about the methods used are given in Ref. [3]. The expected number of background events and the number of observed events are summarised in Table 1.

Table 1: The expected number of background events and the number of observed events after the full selection [3]. The quoted uncertainties are statistical only. The notation ℓ stands for e and μ only.

	$\tau_\mu\tau_{\text{had}}$ (1.55 fb^{-1})	$\tau_e\tau_{\text{had}}$ (1.34 fb^{-1})	$\tau_e\tau_\mu$ (1.55 fb^{-1})
$\gamma^*/Z \to \ell\ell$	81 ± 7	64 ± 4	23 ± 4
$W \to \ell\nu$	186 ± 13	45 ± 5	<0.5
$W \to \tau\nu$	49 ± 5	18 ± 2	<0.5
$t\bar{t}$	31 ± 1	17 ± 1	2 ± 1
Diboson	15 ± 2	6 ± 1	18 ± 2
Multijet	432 ± 30	300 ± 21	13 ± 7
Total background	793 ± 34	449 ± 22	56 ± 8
$\gamma^*/Z \to \tau\tau$	4544 ± 49	2029 ± 25	981 ± 26
N_{obs}	5184	2600	1035

4. Cross section measurement and results

The measurement of the cross section is done separately in each channel and the obtained values are then combined. The calculation is performed using the formula

$$\sigma(Z \to \tau\tau, m_{\tau\tau} \in [66,116]\ \text{GeV}) \times \text{B} = \frac{N_{\text{obs}} - N_{\text{bkg}}}{A_Z \cdot C_Z \cdot \mathscr{L}} \tag{4.1}$$

where N_{obs} is the number of observed events, N_{bkg} is the number of estimated background events, B is the branching fraction for the channel considered and $\mathscr{L}$ denotes the integrated luminosity for

the final state of interest. A_Z is the geometrical and kinematic acceptance factor for events with the $\tau\tau$ invariant mass between 66 GeV and 116 GeV. C_Z stands for the experimental correction factor which accounts for the efficiency of triggering, reconstructing and identifying the $Z \to \tau\tau$ events.

Several sources of systematic effects have been studied. The dominant systematic uncertainties contributing in all three channels are the energy scale, luminosity and A_Z uncertainty. Furthermore, the tau identification leads to a large uncertainty in the $\tau_\mu \tau_{\text{had}}$ and $\tau_e \tau_{\text{had}}$ channels, the tau trigger efficiency and electron identification efficiency in the $\tau_e \tau_{\text{had}}$ channel. The measured cross sections with their statistical and systematic uncertainties are summarised in Table 2.

Table 2: The production cross section times branching fraction for the $Z \to \tau\tau$ processes measured in each final state [3].

Final State	$\sigma(Z \to \tau\tau, m_{\tau\tau} \in [66,116]\ \text{GeV})$
$\tau_\mu \tau_{\text{had}}$	$0.91 \pm 0.01(\text{stat}) \pm 0.09(\text{syst}) \pm 0.03(\text{lumi})$ nb
$\tau_e \tau_{\text{had}}$	$1.00 \pm 0.02(\text{stat}) \pm 0.13(\text{syst}) \pm 0.04(\text{lumi})$ nb
$\tau_e \tau_\mu$	$0.96 \pm 0.03(\text{stat}) \pm 0.09(\text{syst}) \pm 0.04(\text{lumi})$ nb

The individual results are combined by means of the BLUE (Best Linear Unbiased Estimate) method [5, 6] leading to the value of $\sigma(Z \to \tau\tau) = 0.92 \pm 0.02(\text{stat}) \pm 0.08(\text{syst}) \pm 0.03(\text{lumi})$ nb. The individual cross sections together with the combined result are shown in Figure 4. The theoretical expectation [7, 8, 9] of 0.96 ± 0.05 nb is also shown.

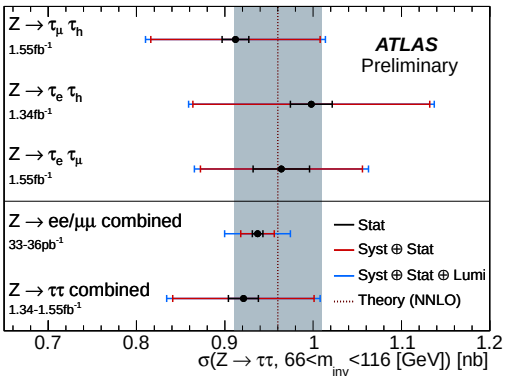

Figure 4: The $Z \to \tau\tau$ individual cross section measurements and the combined result [3]. The $Z \to \ell\ell$ combined cross section measured by ATLAS [10] is shown for comparison. The grey band indicates the uncertainty on the NNLO cross section prediction.

5. Variables used in the hadronic τ identification

The sample obtained after the full selection in the $\tau_\mu \tau_{\text{had}}$ has a relatively high purity in hadronic τ decays allowing a study of the variables used by the τ identification for signal-like τ candidates. As an example, a calorimeter cluster mass (defined in Ref. [1]) is shown in Figure 5 (a) and the distribution of the Boosted Decision Tree (BDT) score [11, 12, 1] before any identification require-

ments on the τ candidate have been applied in Figure 5 (b). More distributions are compared in Ref. [3] and in general, a good agreement between data and Monte Carlo is observed.

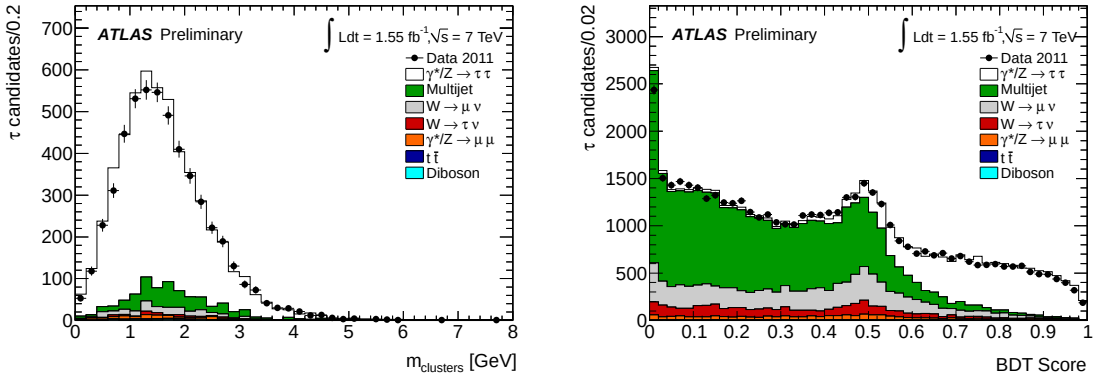

(a) $\tau_\mu \tau_{\text{had}}$ channel (b) $\tau_\mu \tau_{\text{had}}$ channel

Figure 5: Variables relevant for the hadronic τ identification: (a) calorimeter cluster mass and (b) distribution of the BDT score [3].

6. Summary

The measurement of the $Z \to \tau\tau$ cross section with the ATLAS detector using collision data collected at the centre-of-mass energy of 7 TeV corresponding to the integrated luminosity of $1.34 - 1.55$ fb^{-1} has been presented. The measurements are performed in three channels ($\tau_\mu \tau_{\text{had}}$, $\tau_e \tau_{\text{had}}$ and $\tau_e \tau_\mu$) and the individual results are combined together resulting in the total cross section of $0.92 \pm 0.02(\text{stat}) \pm 0.08(\text{syst}) \pm 0.03(\text{lumi})$ nb which is in a good agreement with the theoretical predictions and previous measurements.

The obtained sample after all selections has a high purity of τ leptons and is used to study a number of variables relevant to the identification of hadronic τ decays. A good description of these variables by the Monte Carlo simulation is observed.

References

[1] ATLAS Collaboration, ATLAS-CONF-2011-152, http://cdsweb.cern.ch/record/1398195.
[2] ATLAS Collaboration, 2008 JINST **3** S08003.
[3] ATLAS Collaboration, ATLAS-CONF-2012-006, http://cdsweb.cern.ch/record/1426991.
[4] Particle Data Group Collaboration, J. Phys. **G37** (2010) 075021.
[5] L. Lyons, D. Gibaut, and P. Clifford, Nucl. Instrum. Meth. **A270** (1988) 110.
[6] A. Valassi, Nucl. Instrum. Meth. **A500** (2003) 391 – 405.
[7] K. Melnikov and F. Petriello, Phys. Rev. **D74** (2006) 114017.
[8] R. Gavin, Y. Li, F. Petriello, S. Quackenbush, Comput. Phys. Commun. **182** (2011) 2388 – 2403.
[9] S. Catani, L. Cieri, G. Ferrera, D. de Florian and M. Grazzini, Phys. Rev. Lett. **103** (2009) 082001.
[10] ATLAS Collaboration, Phys. Rev. **D85** (2012) 072004.
[11] L. Breiman, J. Friedman, C. Stone, and R. Olshen, Chapman & Hall, 1984.
[12] Y. Freund and R. Shapire, Proceedings 13th International Conference on Machine Learning, 1996.